ACCEPTED VERSION, the published version is available under Elsevier copyright at 10.1016/j.electacta.2022.141780

Article

Waste Carbon Ashes/PEDOT:PSS Nano-Inks for Printing of Supercapacitors

Antonella Giuri[1,2]*, Raffaella Striani[1], Sonia Carallo[2], Silvia Colella[3], Aurora Rizzo[2], Claudio Mele[1], Sonia Bagheri[1], Miriam Seiti[4], Eleonora Ferraris[4] and Carola Esposito Corcione[1,2]

[1] Università del Salento, via per Monteroni, km 1, I-73100, Lecce, Italy; antonella.giuri@unisalento.it; raffaella.striani@unisalento.it; claudio.mele@unisalento.it ; carola.corcione@unisalento.it; sonia.bagheri@unisalento.it
[2] CNR-NANOTEC-Istituto di Nanotecnologia, Polo di Nanotecnologia, c/o Campus Ecotekne, via Monteroni, I-73100 Lecce, Italy; antonella.giuri@nanotec.cnr.it ; aurora.rizzo@nanotec.cnr.it; sonia.carallo@nanotec.cnr.it
[3] CNR NANOTEC - c/o Dipartimento di Chimica, Università di Bari, Via Orabona 4, 70126 Bari, Italy; silvia.colella@nanotec.cnr.it
[4] Department of Mechanical Engineering, Campus de Nayer, KU Leuven, 2860 Sint-Katelijne-Waver, Belgium; miriam.seiti@kuleuven.be; eleonora.ferraris@kuleuven.be

Abstract: The aim of this paper is the development of an innovative method for the recycling of carbon-based ashes waste derived from the production plant CMD ECO 20, designed by the company Costruzioni Motori Diesel (C.M.D.) for the combined production of electricity and heat.
In this work we propose, for the first time, an original way for a technological/industrial valorisation of the carbon ashes waste, produced from biomass pyro-gasification plant, by using them as fillers of electrically conductive inks suitable for the fabrication of supercapacitors. A water-based dispersion containing nanometric waste carbon ashes (nCA), of around 300 nm, was obtained from carbon waste ashes of wooden biomass through an eco-friendly process.
The developed inks based on PEDOT:PSS and nCA showed good capacity performance, explored by cyclic voltammetry (CV) measurements, with CV characterised by approximately rectangular shape and long-term stability in the time. Indeed the best specific capacitance of 26.80±0.21 F/g, achieved for the nCA0.5PEDOT:PSS film was retained at 96.8% of the initial capacitance after 1000 cycles. The PEDOT:PSS/ nCA based suspensions were then characterised by rheological and surface tension analysis, as a function of the nCA concentration ahead of printing deposition with the aim to investigate the printability of the developed inks.Finally, the printability of the inks was investigated and demonstrated by means of Aerosol Jet Printing (AJ®P) setup with the aim to identify a production technology suitable for their use in printed electrical applications.

Keywords: Carbon based ashes/PEDOT nanocomposite, Aerosol Jet® printing, supercapacitors, circular economy, recycling

---

1. Introduction

The increase in the amount of waste and greenhouse gases emissions, as well as the scarcity of resources, caused by the current economic development model (i.e. Linear Economy), are heavily threatening the stability of the economies and integrity of the natural ecosystems. Hence, in order to decrease the consumption of primary energy and raw materials and the production of waste, a transition from the Linear to Circular Economy has become necessary.

In this context, several companies have put in place the so-called Zero Emissions Strategy which aims at reducing primary energy consumption as well as greenhouse gas emissions, by employing renewable energy sources. The Italian company Costruzioni Motori Diesel S.p.A. (CMD) has put in place this strategy by developing a pyro-gasification plant, CMD ECO 20, which produces electric and thermal power via thermo-chemical decomposition or molecular dissociation of lignocellulosic biomass, even waste biomass (e.g., agricultural residues) at high temperature (from 600 to 1000 °C), and in complete absence or minimum quantities of oxygen (pyro-gasification). This emerging technology improves the efficient use of energy and reduces the environmental impact, by mitigating the consumption of primary energy and emission of the associated greenhouse gas. However, this system also produces waste, in the form of carbon-based ashes (CA), which, according to the European List of Wastes (Commission Decision 2000/532/EC)[1,2], are classified as a solid product to be disposed of in landfills or ash ponds. The CA disposal in landfill constitutes a considerable economic burden for the company as well as it can cause long-term negative effects on the environment and human health.

The CA are introduced especially into the environment through the transport from the plant site to the landfill or ash pond [3], contributing to the formation of particulate matter (PM) [4]. The PM absorbs many pollutants, such as nitrogen dioxide (NO_2), from the air, causing several diseases, including asthma, chronic obstructive pulmonary disease, and cardiac arrhythmias, as well as a higher rate of infant mortality [5]. In addition, the PM toxicity increases when polycyclic aromatic hydrocarbons (PAHs) are released during the fuel combustion, and it is known that the inhalation of PAHs causes negative effects on the neurological development of the children [6]. The PAHs also produce reactive electrophilic species which react with the nucleobases of the DNA causing genetic mutations, cancer, and different cardiovascular diseases [7]. Therefore, the goal of this paper is to propose innovative solutions for recycling CA produced by the (pyro-) gasification process of biomass of the company CMD (and by combustion in general), with consequent increase of the efficiency of company waste management and reduction of its negative effects on environment and human health. The possibility to produce valorised materials, obtained starting from waste materials, recently attracted the attention of both academic and industrial researchers. The circular economy has, in fact, grown in importance in academic study over the previous decade, with a significant increase in the number of publications and journals dedicated to the subject. A key development goal of the circular economy is the reuse of different kinds of wastes, particularly wastes from industrial operations. The passage from Linear to Circular Economy, in fact, presupposes a change of collective mentality, which includes governments, companies and individuals, about the way we produce and consume, in order to extend the life cycle of the products and, as a consequence, decrease the consumption of primary energy and resources, and the production of waste. Several researchers have been studying the potential and valorisation of the ashes in a circular economy scenario. Currently, the potential re-uses of carbon-based waste ashes mostly include soil amendment and fertilisation methods, followed by the production of construction materials and sorbents, and the synthesis and production of ceramics and other materials [8–13]. In previous works, the authors have also explored different way to recycle these waste ashes: i) as catalysts for the crosslinking (cure) reaction of diglycidyl ether of bisphenol A (DGEBA) with a diamine, observing a reduction in the curing time along with an increase of the flexural properties and the glass transition temperature of the epoxy resin [14]; ii) as reinforcing fillers in thermoplastic starch (TPS) films for agricultural applications, observing improved thermal and durability performances of the TPS films in outdoor conditions. In addition, the waste carbon ashes/maize starch films can release plant nutrients contained in the ashes into the soil, after degradation, with respect to the neat starch [15,16]. Moreover, an original procedure to reduce the dimensions of the waste ashes in an aqueous solution for the development of printed electronics (PE) inks was put in place by the authors in a previous work [17]. Printability via Aerosol Jet® Printing (AJ®P) was also verified preliminary. AJ®P is a direct-writing additive manufacturing technique which has been introduced by Optomec Inc. (USA) in the early 90s especially for printing of electronics. Since then, its abilities have been exploited for the production of passive and active elements. In recent years, the technology has been also exploited for surface structuring and biological interfaces, including bioelectronic constructs. Its use is crucial here since nCA are in a diluted water-based dispersion with a final composite inks low viscosity in the range of 0.004 to 6 Pas. Therefore, this technology is preferred over more conventional and higher throughput methods, such as screen printing, which requires the use of thicker paste-like dispersions. Moreover, contrary to ink-jet printing techniques, AJ®P has the advantage to achieve high resolutions (down

to 20 microns in width and 100 nm in thickness) on free-form substrates (rigid, flexible, 2D and 3D shapes) due to a variable stand-off distance (i.e. the distance between the tip of the nozzle and the substrate) from 1 to 5 mm. Eventually, the technique in its ultrasonic configuration, gives the opportunity to print a wide range of water-based inks, from 0.001 to 1 Pas in viscosity, with a particle size < 0.5 micron.

The use of recycled carbon based materials for electrical application is of large interest in the literature: such as for i) Pet coke, transformed into Pet graphene, to develop renewable energy storage devices like supercapacitors [18]; ii) porous graphitic carbon synthesised from an invasive plant 'Eichhornia crassipes' to fabricate hole transport material/counter electrode for perovskite based solar cells[19]; iii) smoking ash as energy storage material [20]; and iv) biochar, produced through the carbonization of infested ash tree residues, as a potential active material for supercapacitor electrodes[21,22].
Encouraging by these works and considering the promising authors' preliminary results mentioned above, the recycling of the carbon waste ashes as fillers in poly(3,4-ethylenedioxythiophene) polystyrene sulfonic acid (PEDOT:PSS) based conductive inks for Aerosol Jet® is, here, further explored. In particular, PEDOT:PSS is a conjugated polymer characterised by an electrical conductivity ranging from 10^{-5} to 1 S/cm, based on the PEDOT/PSS ratio [23], and widely used in the electronic field. Sometimes, a secondary doping of PEDOT:PSS is necessary to increase its electrical conductivity properties.
In the last few years, nanosized carbon-based fillers, such as graphene and carbon nanotubes (CNTs), have been successfully explored to develop PEDOT:PSS based composites, with enhanced electrical conductivity[24]. As an example, in one of our previous paper [25], glucose (G), α-cyclodextrin (α-CD) and sodium salt of carboxymethyl cellulose (CMCNa) were used as dispersing agents for graphene oxide (GO), exploring the influence of both saccharide units and geometric/steric hindrance on the rheological, thermal, wettability and electrochemical properties of a GO/PEDOT:PSS nanocomposite. The electrochemical properties of the GO/ PEDOT composites with different dispersing agents for supercapacitors were investigated using cyclic voltammetry (CV). The CV results revealed that GO/PEDOT with glucose exhibited the highest specific capacitance among the systems investigated. The capacitive performance of PEDOT:PSS and of GGO-PEDOT was also investigated by means of cyclic voltammetry (CV) under UV ageing, demonstrating a good conductive behaviour, with a specific capacitance of 16 F/g, and stability of the films under UV treatment of 4 hours[26]. Motivated by these interesting results, in this paper the possibility to substitute the GO fillers with the nanometric carbon-based wastes is explored, for the first time. Moreover, the feasibility to obtain innovative PEDOT:PSS/nCA based nanocomposite supercapacitors to fabricate by Aerosol Jet printing is investigated.

2. Materials and Methods

Carbon-based ashes (CA), provided by the company Costruzioni Motori Diesel S.p.A. (CMD), are the by-product of the biomass pyro-gasification plant CMD ECO20.
PEDOT:PSS aqueous solution (Orgacon® IJ 1005), composed by PEDOT:PSS concentration of 0.8% by weight and 10-20 wt.% of diethylene glycol, was purchased from AGFA NV, BE.

2.1 nCA production

A water solution of nanometric CA, with a concentration of 0.4 wt.%, was obtained following the method previously developed [17]. In detail, the reduction of the carbon-based ashes size towards the nanometre scale in an aqueous solution was demanded by the AJP technique constraints (working with nanometric solutions only), and carried out by means of a multistep reduction size process, that consisted of ball milling and sonication techniques. The distribution of the treated CA ashes was monitored by multi-angle laser scattering (MALS) (CILAS1190 particles size analyser) (CPS Us, Inc., Madison, WI, USA) and by dynamic light scattering (DLS Zetasizer-Malvern) (Malvern Panalytical Ltd, Malvern, UK). The optimised method has resulted in stable and homogeneous aqueous dispersions with 98.4% of distribution of nCA particles characterised by diameter equal to 331.3± 188.7nm, as reported in Scheme I. This method presents several advantages, such as the possibility to obtain stable and reproducible water dispersed nanometric CA-based inks in a short time. A further advantage is the production of carbon-based nanoparticles dispersed in a green solvent (water). In

addition, this procedure allows the production of large amounts (about 5 L) of nanometric water-based dispersions. However, the yield of this process is still too low, and this aspect requires further studies.

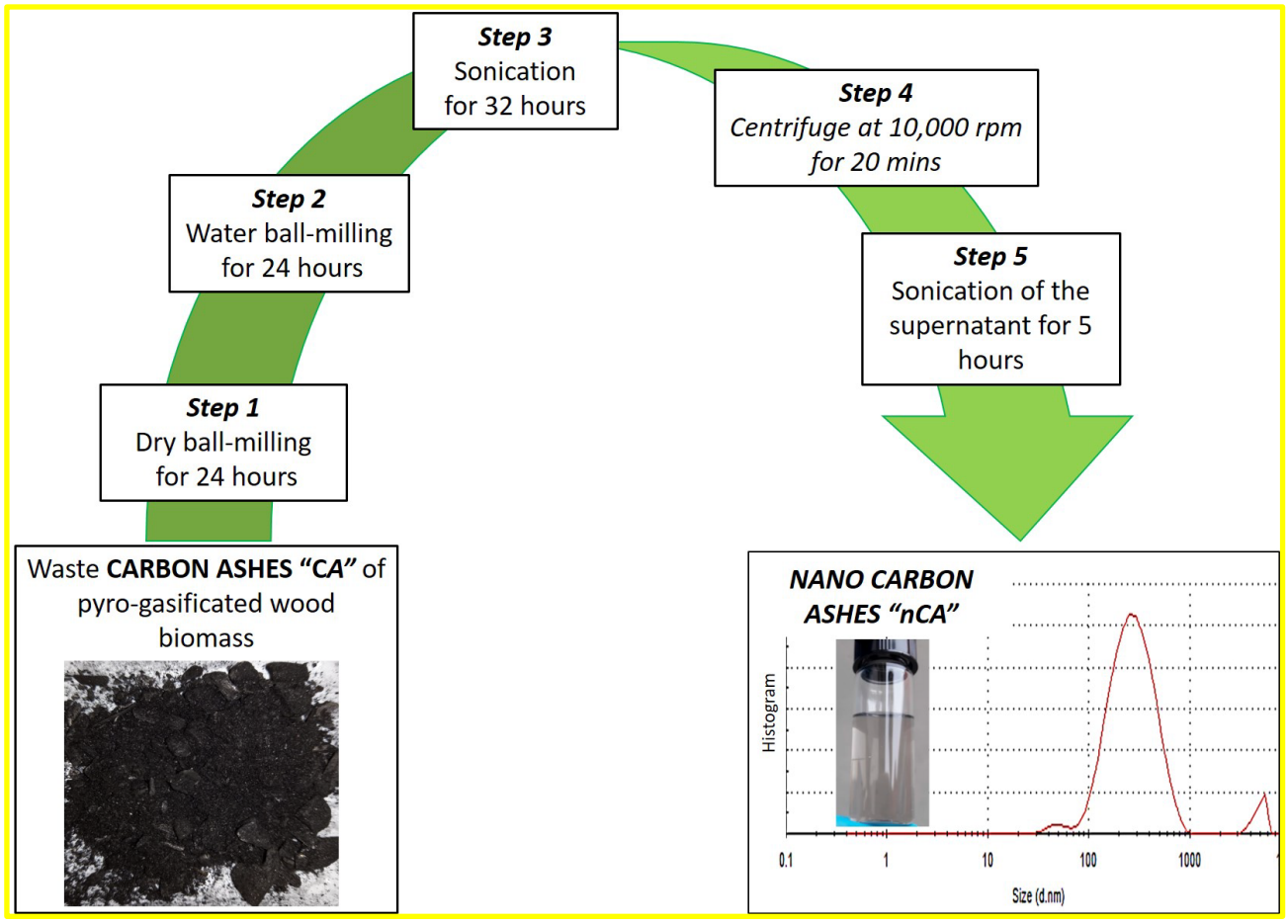

Scheme I. Method for nanometric carbon ashes production

2.2 PEDOT:PSS + nCA nanocomposite solution preparation

The dispersion of nCA solutions into the PEDOT:PSS was obtained by the solvent swelling method, developed in the previous works[25,26]. The nCA solutions (0.4 wt.%/water) were added into PEDOT:PSS with a final nCA concentration of 0.1%, 0.2% and 0.5% wt/$V_{PEDOT:PSS}$ and the solutions were stirred for 90 minutes and sonicated for 15 min at room temperature. The prepared solutions, with the respective ID, are reported in Table 1.

Table 1. nCA/PEDOT:PSS inks composition

Sample	nCA %wt/$V_{PEDOT:PSS}$
PEDOT:PSS	0
nCA0.1 PEDOT:PSS	0.1
nCA0.2 PEDOT:PSS	0.2
nCA0.5 PEDOT:PSS	0.5

2.3 nCA morphological characterization

Morphological analysis of the nCA was recorded via SEM. Samples were made by dropping the nCA water solutions on an ITO substrate and dried in ambient air to remove the water and exposed the dried powders. SEM images were acquired by using a ZEISS Sigma 300 VP (Field Emission Scanning Electron Microscope) instrument in high vacuum and high-resolution mode, equipped with a Gemini column and an integrated high efficiency in-lens detector. The applied acceleration voltage was 5 kV.

2.4 PEDOT:PSS + nCA nanocomposite film electrochemical characterization

Electrochemical measurements were carried out with a PARSTAT 2273 potentiostat/galvanostat. A three-electrode electrochemical cell was employed. As working electrodes we investigated four films of PEDOT:PSS, nCA0.1PEDOT:PSS, nCA0.2PEDOT:PSS and nCA0.5PEDOT:PSS, obtained by drop casting of the prepared inks described above on a platinum disc (diameter 2 mm) embedded in a Teflon cylindrical holder, followed by evaporation in air. A platinised titanium expanded mesh electrode was used as a counter electrode and a Ag/AgCl (KCl 3 M) was employed as reference electrode; potential values were reported vs. Ag/AgCl. The capacitive performance of PEDOT:PSS based films as materials for supercapacitors was investigated in a 1 M H_2SO_4 aqueous solution at room temperature by means of cyclic voltammetries (CVs), performed at different scan rates between 5 and 100 mV/s, in the potential range from -0.2 V to 0.8 V. Each measurement was repeated three times.

2.5 PEDOT:PSS + nCA nano-inks characterization

The viscosity of all the inks was carried out in a strain controlled rheometer (Malvern Kinexus Pro+) equipped by parallel plate geometry (radius = 12.5 mm) in steady state mode with a shear rate ranging from 0.1–1000 s−1 at 20 °C. All measurements were made in triplicate. According to the Cross model (Eq. 1) [27] the plateau values for the lower (η_0) and upper (η_∞) Newtonian viscosities, was predicted:

$$\eta = \eta_\infty + [\eta_0 - \eta_\infty / 1 + (\tau \gamma_0)^m] \quad (1)$$

where τ corresponds to the reciprocal of the shear rate at which the calculated value of η equals η_0, γ_0 is the value of the shear rate equal to zero, while the parameter m is related to the power low index n (m=n-1) .

Surface tension. The surface tension of the inks was evaluated by using a drop shape analyser FTA1000. All measurements were made in triplicate.

2.6 Aerosol Jet® Printing of PEDOT:PSS + nCA nano-inks

The industrial processability of the developed nano-inks was also verified via AJ®P. Prior printing, the nano-inks (each one of ~1 mL) were sonicated in an ultrasonic bath (EMMI - 20 HC, Emag) at T = 25°C for 10 min. Furthermore, the inks were ultrasonically atomized in an AJ®P setup (300s system, Optomec, USA) at a power of 49.5 V. Based on previous expertise with the AJ®P of the same PEDOT:PSS ink without nCA composite[28], the print parameters were investigated and eventually set at a carrier gas flow, *CGF* = 40 sccm, a sheath gas flow, *SGF* = 80 sccm, a platen temperature, *T* = 40 °C, a print speed, *s* = 15 mm/s, and at an offset (e.g. distance from the nozzle exit to the substrate), *z* = 3 mm. For each ink, 3 repetitive squares of 8 x 8 mm (interlayer spacing of 0.08 mm) were printed at a print layer, *n*, equal to 20. Glass slides (Superfrost, VWR, BE) were used as substrate, after being ultrasonically cleaned (T = 25°C, 10 mins) with distilled water (DI) and 2-propanol (IPA, Sigma Aldrich, BE). Final AJ®P films were annealed in a thermal oven at 150 °C for 45 minutes (Heraeus, DE) to allow co-solvents evaporation. The morphology of PEDOT:PSS + nCA nanocomposite film printed by AJ®P on glass substrate was analysed by SEM.

3. Results and discussion

The morphological characterization of nCA confirms a large distribution of nanometric fragments, sometimes characterised by shape close to sheets, with size lower than about 400 nm, compared to hundreds of

micrometres of the CA fragments before reduction process (Figure 1). It is also evident the presence of micrometres size clusters with irregular shape randomly distributed in the sample, maybe due to the deposition of the dispersion by drop casting.

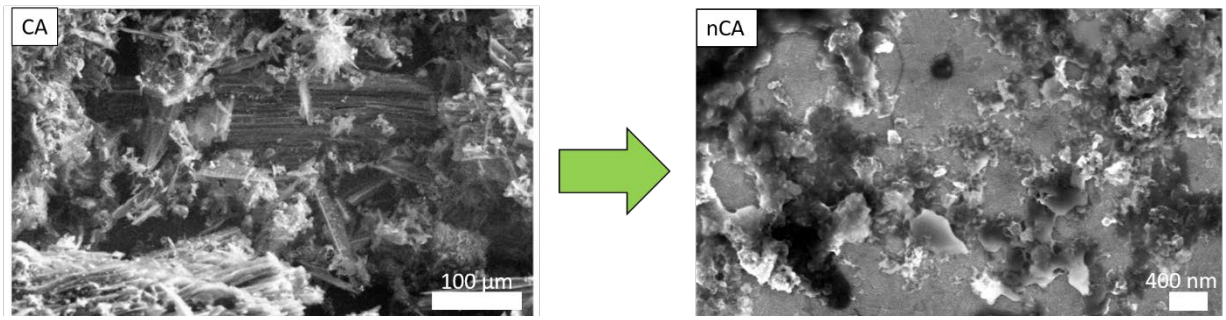

Figure 1. Morphological characterization of carbon ashes fragment before reduction process (a) and nano carbon ashes (b)

The capacitive performance of PEDOT:PSS/nCA based inks was explored by cyclic voltammetry (CV) measurements. In fact, PEDOT:PSS has been reported in the many literature works (i.e. [29-33]) as efficient material for supercapacitors. The capacitance of PEDOT:PSS/carbon-based composites can be improved thanks to the increased surface area that magnifies the Faradaic interactions between composites and electrolyte [33] and the challenge in fabricating these composites is also achieving the correct ratio of the materials [29-32]. Figure 2(a) reports the specific current (i.e referred and normalised to 1 g of active material) measured by CVs at a scan rate of 100 mV/s in a 1 M H_2SO_4 solution for the four films prepared according to the procedure described in Section 2.4.

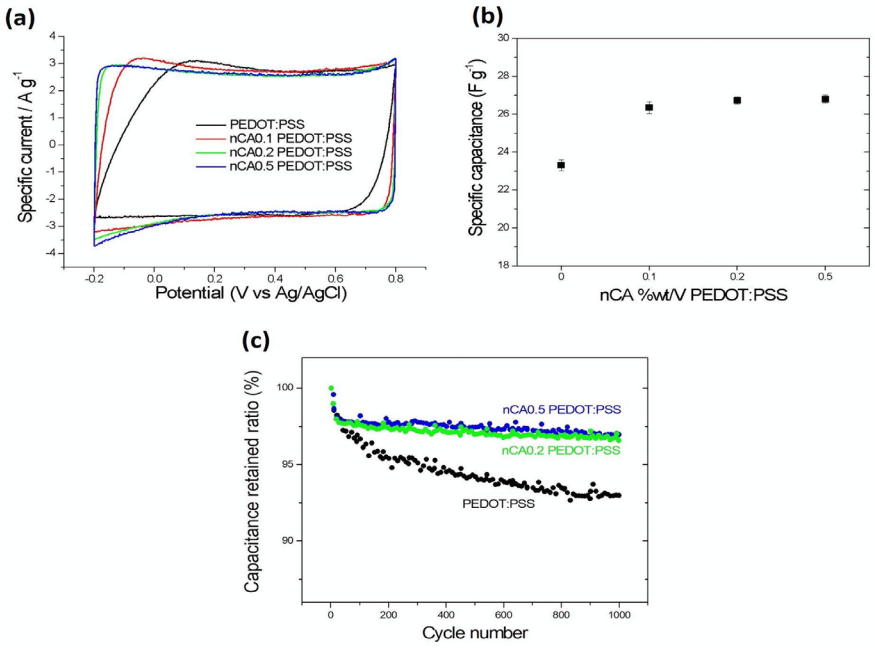

Figure 2. Cyclic voltammograms at a scan rate of 100 mV/s for the four PEDOT:PSS based films in 1 M H_2SO_4 aqueous solution at room temperature (a); Specific capacitance estimated from CVs (b); Specific capacitance as a function of the cycle number for PEDOT:PSS, nCA0.2PEDOT:PSS and nCA0.5PEDOT:PSS films (c).

The CVs of the films present a broad, approximately rectangular shape, due to a large double-layer capacitance. The best rectangular shape is observed in particular for the nCA0.5PEDOT:PSS film. As described in the literature [26,34,35], the enclosed area of CV curves, which corresponds to the charge storage capacity of the electrodes, depends strongly on the material properties.

For a quantitative assessment of the functional performance of the four films, their specific capacitance C_{sp} was estimated by means of Equation 2 [36]:

$$C_{sp} = \frac{\int idV}{2 \cdot m \cdot \Delta V \cdot s} \quad (2)$$

where $\int idV$ is the integrated area of the CV, m is the mass of the electrode material (g), *s* indicates the scan rate (V s^{-1}) and ΔV is the range of applied potential (V). The C_{sp} values calculated from CVs at a scan rate of 100 mV/s for the four investigated materials are plotted in Figure 2(b). For the PEDOT:PSS film prepared without additives, C_{sp} is 23.31±0.29 F/g and is consistent with literature data [26,33]. For the films containing nCA, C_{sp} is higher and increases with the amount of nCA, reaching the values of 26.35±0.30, 26.73±0.19, and 26.80±0.21 F/g for the PEDOT:PSS film with nCA0.1, nCA0.2 and nCA0.5, respectively. The error bands reported in the figure correspond to the variation of the specific capacity measured values, obtained by repeating three times the tests with three different films prepared independently for each investigated composition.

The electrochemical stability of the films was evaluated by repeating in some representative conditions the CV test for 1000 cycles [34, 37, 38]. Fig. 2c shows the relative change of the specific capacitance for PEDOT:PSS, nCA0.2PEDOT:PSS and nCA0.5PEDOT:PSS films, as a function of the cycle number, measured from CVs obtained at 100 mV/s. A slow gradual decrease was observed with a satisfactory cyclic stability, since after 1000 cycles 93.0%, 96.6% and 96.8% of the initial capacitances were retained for PEDOT:PSS films, without nCA and with nCA0.2 and nCA0.5, respectively. The addition of nCA is therefore attractive for improving the long-term stability of PEDOT which, although satisfactory, could be limited because of shrinkage, breaking, and cracks appearing often in conducting polymers in a sequence of many cycles [39, 40]. These problems are connected with volumetric changes of the polymer during the intercalation and deintercalation of counter ions [32]. From our results, the addition of a small quantity of nCA was proved to reduce the slow degradation in capacitance. This positive result could be due to a synergistic effect of PEDOT:PSS and nCA with a large accessible specific surface area and increased electroactive binding sites for electrolyte ions during the charge-discharge process, giving rise to superior cyclic performance [41].

In order to investigate more in detail and to confirm the observed effect of the addition of nCA, further analyses were performed by assessing the specific capacitance of the films at different scan rates. The specific current obtained by CVs at different scan rates between 5 and 100 mV/s, for PEDOT:PSS and nCA0.5PEDOT:PSS films is reported in Figure 3(a) and (b).

The specific voltammetric charge C_{vc} was evaluated by means of Equation 3:

$$C_{vc} = \frac{\int idV}{2 \cdot m \cdot \Delta V} \quad (3)$$

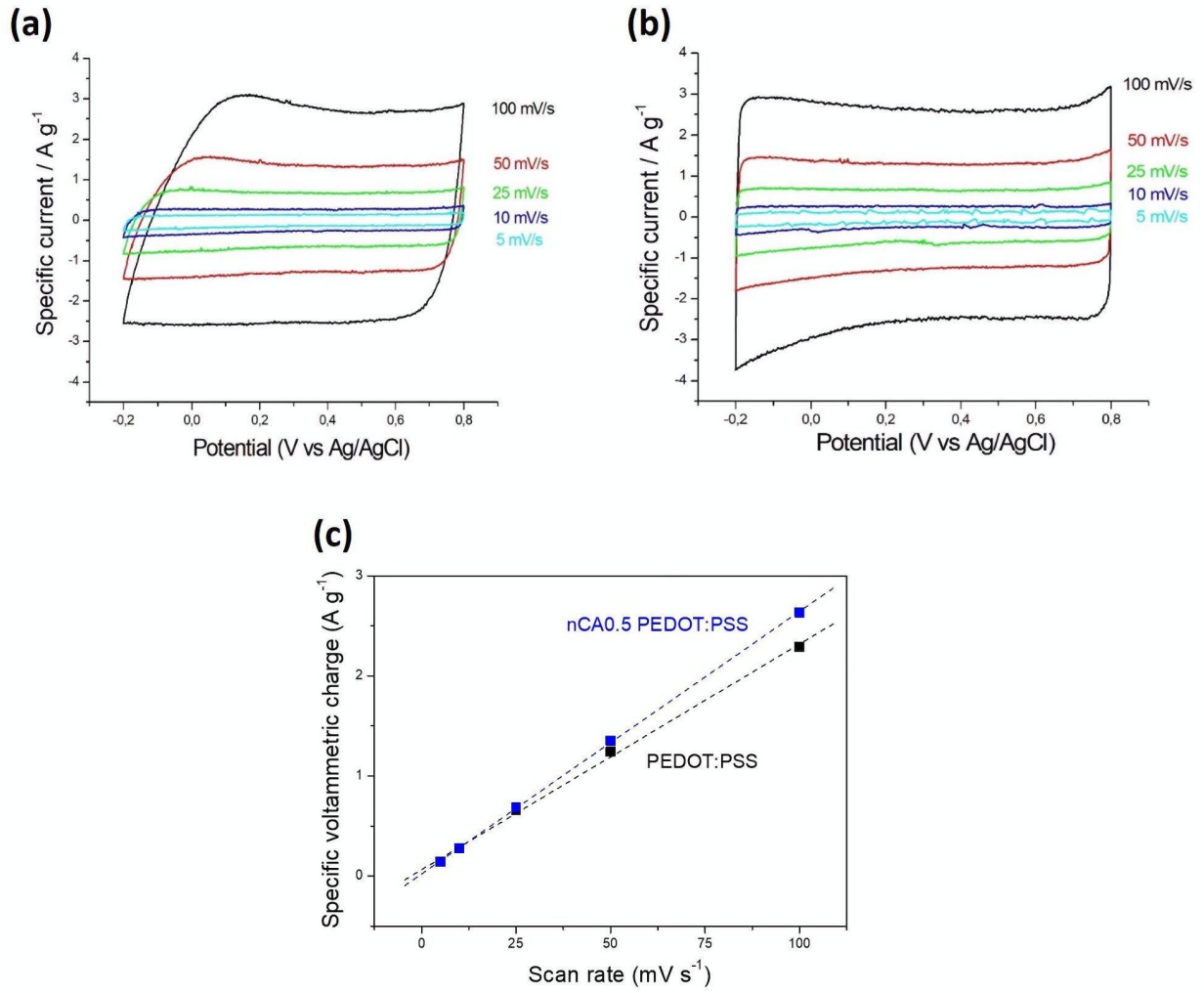

Figure 3. Cyclic voltammograms at different scan rates for PEDOT:PSS (a) and nCA0.5PEDOT:PSS films in 1 M H_2SO_4 aqueous solution at room temperature (b);specific voltammetric charge as a function of scan rate for PEDOT:PSS and nCA0.5PEDOT:PSS films (c). Dashed lines represent the linear fit whose slope is the specific capacitance C_{sp}.

In Figure 3(c), C_{vc} was reported as a function of the scan rate for PEDOT:PSS and nCA0.5PEDOT:PSS films. Dashed lines represent the linear fit whose slope is the specific capacitance C_{sp} [42]. C_{sp} values of 22.53±0.56 and 26.20±0.19 F/g were obtained in the absence of nCA and with nCA0.5, respectively.

These results reveal a good capacitive behaviour of the prepared films, indicating as these materials are potentially suitable to be used as electrode material for supercapacitors and as the performance of PEDOT:PSS film can be improved by the addition of the appropriate amount of nCA. In our study, nCA0.5PEDOT:PSS film showed the best performance among the investigated films. The high capacitance of nanometric carbon ashes/PEDOT:PSS nanocomposites can be related to the very large surface area of nCA which magnifies the Faradaic interactions between composites and electrolyte [43, 44].

With the aim to investigate the printability of the inks by AJ®P, rheological and surface tension measurements were carried out on the developed inks as reported in Figure 4. From the analysis of the steady state viscosity measurements, reported in Figure 4(a), the PEDOT:PSS shows a reduction in viscosity as a function of the shear rate, typical of pseudo-plastic behaviour, with viscosity values ranging from about 1.2 Pa s at 0.1 s^{-1} to 0.01 Pa s at 1000 s^{-1}. After nCA addition, the rheological behaviour of the inks is still pseudo-plastic, irrespective of the amount of nCA. The viscosity value remains the same at low shear rate, 0.1 s^{-1}, instead decreasing down to 0.005 Pa s with 0.1 wt.% and to 0.004 Pa s with 0.2 and 0.5 wt.% of nCA, at a shear rate of

1000 s^{-1} showed a slight lubrificant effect filler-induced, maybe due to the shape of the nCA close to sheet, as evidenced by morphological analysis.

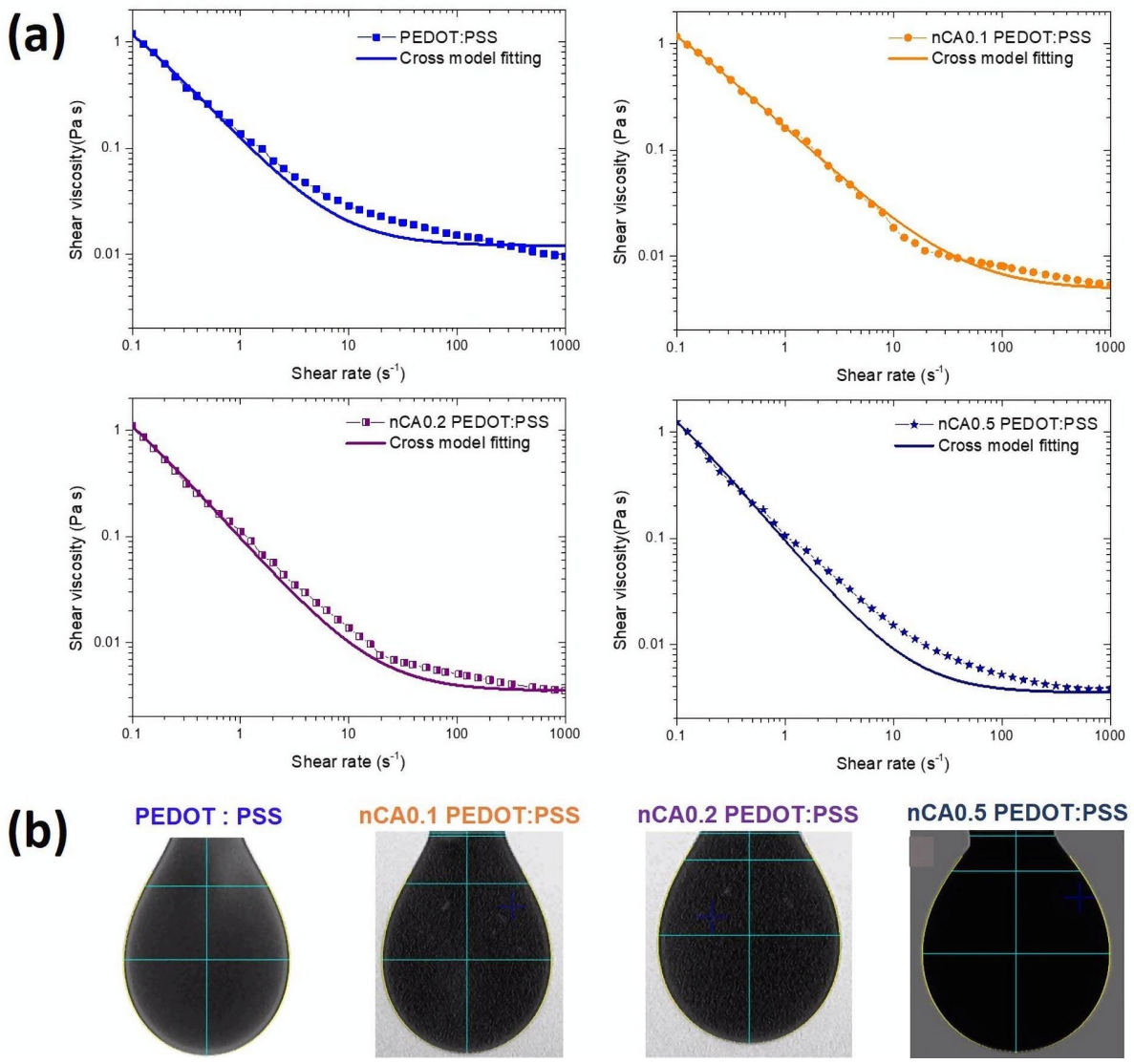

Figure 4. Rheological behaviour and Cross fitting of the nCA/PEDOT:PSS inks (a); surface tension of the nCA/PEDOT:PSS inks (b).

Subsequently, the Cross theoretical model (Eq.1) was applied to fit the experimental data, reported in Figure 4(a), for each sample, to predict the plateau values for lower and upper Newtonian viscosities, η_0 and η_∞ respectively. The values obtained by a nonlinear fitting through the Eq. 1 are reported in table 2, showing a slight increase of the η_0 and decrease of η_∞ by increasing the nCA concentration. The parameter m is very similar for all the samples, meanwhile the values of τ slightly increase after adding the nCA, indicating that the pseudo-plastic behaviour starts at lower shear rate values for the nanocomposite. However, the viscosity values shown by all the samples are within the range of values (0.001-1 Pa s), as required by AJ®P.

Table 2. Parameters of Cross Fitting

Sample	η_0 (Pa s)	η_∞ (Pa s)	τ (s)	m	R^2
PEDOT:PSS	4.5	0.012	25.50	1.13	0.998

nCA0.1 PEDOT:PSS	5.46	0.0048	38.72	0.96	0.999
nCA0.2 PEDOT:PSS	5.47	0.0035	33.66	1.15	0.998
nCA0.5 PEDOT:PSS	6.58	0.0035	32.97	1.22	0.996

The influence of the presence of nCA on the surface tension of PEDOT:PSS was also evaluated and the obtained data are reported in Figure 4(b). The surface tension of the PEDOT:PSS is 31.35±0.9 mN/m, as from values shown in the datasheet. The addition of nCA in an amount of 0.1, 0.2 and 0.5 wt.% increases the surface tension of PEDOT:PSS by about 30, 24 and 42%, respectively. Nevertheless, the surface tensions of each ink (Figure 4(b)) are still compatible with the range of values recommended by the AJ®P (30-40 mN/m). Hence, the inclusion of nCA into the PEDOT:PSS should not change the printability of the pristine ink.

After a proper parameters optimization, the developed inks were successfully ultrasonically atomized in an AJ®P setup, and printed in the form of square samples, as shown in Figure 5(a). The morphology of these samples for different nCA content is also reported in Figure 5(b).

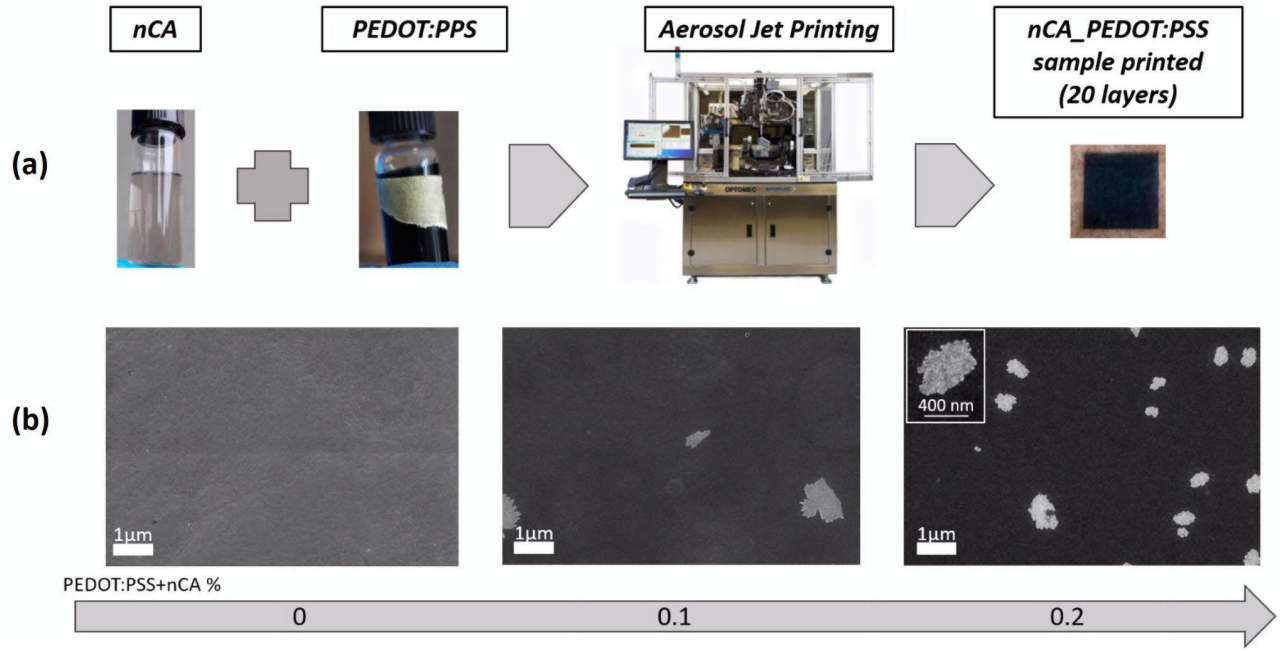

Figure 5. AJ®P process evolution from ink selection to sample printing (a); morphological analyses of the printed samples for different nCA content (b).

Morphological analyses carried out on the printed samples (Figure 5(b)), shows a good dispersion of the nCA filler into the PEDOT:PSS, in particular in the film containing higher nCA content. Moreover, the printed nCA0.2PEDOT:PSS film shows an increased uniformity, with nCA sheets of about 400 nm (in the inset) homogeneously distributed. The lack of micrometres size clusters observed in the pristine nCA may be due to the good dispersion and possibly exfoliation of the ashes into PEDOT:PSS.

4. Conclusions

~~An innovative method for the recycling and valorisation of waste carbon-based ashes was proposed. They were employed as fillers in PEDOT:PSS conductive inks, printable by Aerosol Jet technique, for the production of supercapacitors.~~

An innovative method for the recycling and valorisation of waste carbon-based ashes, as fillers in PEDOT:PSS conductive inks, printable by Aerosol Jet technique, for the production of supercapacitors was proposed. Starting from the results achieved in our previous study, carbon particles with nanometer size of lower than

about 400 nm were produced from carbon waste ashes in aqueous solution and dispersed in a conductive polymer, i.e. poly(3,4-ethylenedioxythiophene) polystyrene sulfonate (PEDOT:PSS), widely used in jet printing of (bio)electronic devices, with the aim to improve its capacitive behaviour.

–The cyclic voltammetry characterization of the films has shown CVs with a broad approximately rectangular shape, due to a large double-layer capacitance. The best rectangular shape is observed in particular for the nCA0.5PEDOT:PSS film, achieving a specific capacitance of 26.80±0.21 F/g, compared to 23.31±0.29 F/g of pristine PEDOT:PSS. In addition, after 1000 cycles, 96.8% of the initial capacitance was retained for nCA0.5PEDOT:PSS film, compared to 93.0% for PEDOT:PSS films. The good capacitive behaviour of the prepared films demonstrated that the performance of PEDOT:PSS can be improved by the addition of the appropriate amount of CA and their potentiality to be used as electrode material for supercapacitors. The addition of nCA is also attractive for improving the long-term stability of PEDOT.

Finally, the prepared inks have been successfully ultrasonically atomized by using Aerosol Jet Printing (AJ®P). The rheological behaviour of the inks (with viscosity values ranging from about 1 to 0.001 Pa s) as well as the surface tension measurements (with viscosity values ranging from about 31 to 44) have shown values within the range required by the AJ®P. A homogenous and stable atomization has been achieved and no visual differences in the mist generated have been detected over the printing period, demonstrating the stability of the inks. Printed films with nCA sheets of about 400 nm uniformly distributed into the PEDOT:PSS matrix have been obtained, opening the path towards the possibility to fabricate printed devices based on the developed nCA based inks. Since exiguous quantities of carbon-based waste ashes (0.1 to 0.5% wt/$V_{PEDOT:PSS}$) have been used in the proposed applications, the findings obtained do not add value to the carbon-based waste even from an industrial point of view, but still contribute to a change of mentality towards the adoption of a development model of Circular Economy.

Author Contributions: "Conceptualization, C.E.C. and E.F.; methodology, A.G.; software, A.G, R. S.; validation, A.R., S.C. and C.M.; formal analysis, S.Ca, S.B.; investigation, R.S., A.G., S.B., S.Ca, M.S.; resources, C.E.C., E.F.; data curation, M.S., A.G.; writing—original draft preparation, A.G., R.S., C.M., C.E.C.; writing—review and editing, E.F., A.R., S.C.; visualization, A.G., R.S., S.C., M.S.; supervision, C.E.C, E.F.; project administration, C. E.C..; funding acquisition, C.E.C. All authors have read and agreed to the published version of the manuscript." Please turn to the CRediT taxonomy for the term explanation. Authorship must be limited to those who have contributed substantially to the work reported.

Acknowledgments: The authors acknowledge Enrica Stasi for experimental support to samples preparation. Moreover, the authors acknowledge the Research Foundation Flanders (FWO) for the doctoral fellowship granted to Miriam Seiti, 1SB1120N.

Conflicts of Interest: "The authors declare no conflict of interest."

References

[1] Espinosa Modolo, R.C.; Silva, T.; Senff, L.; Tarelho, L.A.C.; Labrincha, J.A.; Ferreira, V.M.; Kerber da Silva, L. Bottom Ash from Biomass Combustion in BFB and Its Use in Adhesive-Mortars. *Fuel Process. Technol.* **2015**, *129*, 192–202.

[2] Tarelho, L.A.C.; Teixeira, E.R.; Silva, D.F.R.; Modolo, R.C.E.; Labrincha, J.A.; Rocha, F. Characteristics of Distinct Ash Flows in a Biomass Thermal Power Plant with Bubbling Fluidised Bed Combustor. *Energy.* **2015**, *90*, 387–402.

[3] Raja, R.; Nayak, A.; Shukla, A.; Rao, K.; Gautam, P.; Lal, B.; Tripathi, R.; Shahid, M.; Panda, B.; Kumar, A.; et al. Impairment of Soil Health Due to Fly Ash-Fugitive Dust Deposition from Coal-Fired Thermal Power Plants. *Environ Monit. Assess.* **2015**, *187*, 679-697.

[4] Bignal, K.L.; Langridge, S.; Zhou, J. Release of Polycyclic Aromatic Hydrocarbons, Carbon Monoxide and Particulate Matter from Biomass Combustion in a Wood-Fired Boiler under Varying Boiler Conditions. *Atmos. Environ.* **2008**, *42*, 8863–8871.

[5] Katsouyanni, K.; Touloumi, G.; Samoli, E.; Gryparis, A.; Le Tertre, A.; Monopolis, Y.; Rossi, G.; Zmirou, D.; Ballester, F.; Boumghar, A.; et al. Confounding and Effect Modification in the Short-Term Effects of Ambient Particles on Total Mortality: Results from 29 European Cities within the APHEA2 Project. *Epidemiology.* **2001**, *12*, 521–531.

[6] Edwards, S.C.; Jedrychowski, W.; Butscher, M.; Camann, D.; Kieltyka, A.; Mroz, E.; Flak, E.; Li, Z.; Wang, S.; Rauh, V.; et al. Prenatal Exposure to Airborne Polycyclic Aromatic Hydrocarbons and Children's Intelligence at 5 Years of Age in a Prospective Cohort Study in Poland. *Environ. Health Perspect.* **2010**, *118*, 1326–1331.

[7] Ewa, B.; Danuta, M. Polycyclic Aromatic Hydrocarbons and PAH-Related DNA Adducts. *J Appl Genet.* **2017**, *58*, 321–330.

[8] Vassilev, S. V.; Baxter, D.; Andersen, L.K.; Vassileva, C.G. An Overview of the Composition and Application of Biomass Ash.: Part 2. Potential Utilisation, Technological and Ecological Advantages and Challenges. *Fuel.* **2013**, *105*, 19–39.

[9] Ribeiro, J.P.; Vicente, E.D.; Gomes, A.P.; Nunes, M.I.; Alves, C.; Tarelho, L.A.C. Effect of Industrial and Domestic Ash from Biomass Combustion, and Spent Coffee Grounds, on Soil Fertility and Plant Growth: Experiments at Field Conditions. *Environ. Sci. Pollut. Res.* **2017**, *24*, 15270–15277.

[10] Greinert, A.; Mrówczynska, M.; Szefner, W. Study on the Possibilities of Natural Use of Ash Granulate Obtained from the Combustion of Pellets from Plant Biomass. *Energies.* **2019**, *12*, 2569-2588.

[11] Eliche-Quesada, D.; Felipe-Sesé, M.A.; Martínez-Martínez, S.; Pérez-Villarejo, L. Comparative Study of the Use of Different Biomass Bottom Ash in the Manufacture of Ceramic Bricks. *J. Mater. Civ. Eng.* **2017**, *29, 04017238-1-11*.

[12] Memon, S.A.; Khan, M.K. Ash Blended Cement Composites: Eco-Friendly and Sustainable Option for Utilization of Corncob Ash. *J. Clean. Prod.* **2018**, *175*, 442–455.

[13] Quaranta, N.; Unsen, M.; López, H.; Giansiracusa, C.; Roether, J.A.; Boccaccini, A.R. Ash from Sunflower Husk as Raw Material for Ceramic Products. *Ceram. Int.* **2011**, *37*, 377–385.

[14] Stasi, E.; Giuri, A.; La Villetta, M.; Cirillo, D.; Guerra, G.; Maffezzoli, A.; Ferraris, E.; Esposito Corcione, C. Catalytic Activity of Oxidized Carbon Waste Ashes for the Crosslinking of Epoxy Resins. *Polymers (Basel).* **2019**, *11*, 1011-1025.

[15] Stasi, E.; Giuri, A.; Ferrari, F.; Armenise, V.; Colella, S.; Listorti, A.; Rizzo, A.; Ferraris, E.; Esposito Corcione, C. Biodegradable Compression Molded Composite Films of Thermoplastic Carbon Based Ashes/Maize Starch for Agricultural Applications. *Polymers (Basel).* **2020**, *12*, 524–539.

[16] Giuri A., Colella S., Listorti A., Rizzo A., E.C.C. Biodegradable Extruded Thermoplastic Maize Starch for Outdoor Applications. *J. Therm. Anal. Calorim.* **2018**, *134*, 549–558.

[17] Striani, R.; Stasi, E.; Giuri, A.; Seiti, M.; Ferraris, E.; Esposito Corcione, C. Development of an Innovative and Green Method to Obtain Nanoparticles from Carbon-Based Waste Ashes. *Nanomaterials.* **2021**, *11*, 577-592.

[18] Mandal, D.; Mahapatra, P.L.; Kumari, R. et al. Convert Waste Petroleum Coke to Multi-Heteroatom Self-Doped Graphene and Its Application as Supercapacitors. *Emergent Mater.* **2021**, *4*, 531–544.

[19] Pitchaiya, S.; Eswaramoorthy, N.; Natarajan, M.; Al., E. Perovskite Solar Cells: A Porous Graphitic Carbon Based Hole Transporter/Counter Electrode Material Extracted from an Invasive Plant Species Eichhornia Crassipes. *Sci Rep.* **2020**, *10*, 6835-6851.

[20] Zulfiqar, A.; Muhammad, T.; Chuanbao, C.; Asif, M.; Nasir, M.; Faheem, K.B.; Tanveer, M.; Imran, S.; Muhammad, R.; Faryal, I.; et al. Solid Waste for Energy Storage Material as Electrode of Supercapacitors. *Mater. Lett.* **2016**, *181*, 191–195.

[21] Kouchachvili, L.; Maffei, N.; Evgueniy, E. Infested Ash Trees as a Carbon Source for Supercapacitor Electrodes. *J. Porous Mater.* **2015**, *224*, 979–988.

[22] Shaker, M.; Asghar, A.; Ghazvini, S.; Cao, W.; Riahifar, R.; Ge, Q. Biomass-Derived Porous Carbons as Supercapacitor Electrodes – A Review. *New Carbon Mater.* **2021**, *36*, 546–572.

[23] Fan, X. Doping and Design of Flexible Transparent Electrodes for High-Performance Flexible Organic Solar Cells: Recent Advances and Perspectives. *Adv. Funct. Mater.* **2021**, *31*, 2009399 (1-30).

[24] Kaur, G.; Adhikari, R.; Cass, P.; Bown, M.; Gunatillake, P. Electrically Conductive Polymers and Composites for Biomedical Applications. *RSC Adv.* **2015**, *5*, 37553–37567.

[25] Giuri, A.; Masi, S.; Colella, S.; Listorti, A.; Rizzo, A.; Liscio, A.; Treossi, E.; Palermo, V.; Gigli, G.; Mele, C.; et al. GO/PEDOT:PSS Nanocomposites: Effect of Different Dispersing Agents on Rheological, Thermal, Wettability and Electrochemical Properties. *Nanotechnology.* **2017**, *28*, 174001-174012.

[26] Giuri, A.; Colella, S.; Listorti, A.; Rizzo, A.; Mele, C.; Esposito Corcione, C. GO/Glucose/PEDOT:PSS Ternary Nanocomposites for Flexible Supercapacitors. *Compos. Part B.* **2018**, *148*, 149–155.

[27] Giuri, A.; Masi, S.; Colella, S.; Listorti, A.; Rizzo, A.; Kovtun, A.; Dell'Elce, S.; Liscio, A.; Esposito Corcione, C. Rheological and Physical Characterization of PEDOT: PSS/ Graphene Oxide Nanocomposites for Perovskite Solar Cells. *Polym. Eng. Sci.* **2017**, 57, 546-552.

[28] Seiti, M.; Ginestra, P.; Ferraro, R.; Giliani, S.; Vetrano, R.; Ceretti, E. et al. Aerosol Jet® Printing of Poly(3, 4-Ethylenedioxythiophene): Poly(Styrenesulfonate) onto Micropatterned Substrates for Neural Cells In Vitro Stimulation. *Int J Bioprinting.* **2022**, *8(1)*, 504-520.

[29] Antiohos, D.; Folkes, G.; Sherrell, P.; Ashraf, S.; Wallace, G.G.; Aitchison, P.; Harris, A. T.; Chen, J.; Minett, A. I. Compositional effects of PEDOT-PSS/single walled carbon nanotube films on supercapacitor device performance. *J. Mater. Chem*. **2011**, 21, 15987-15994.

[30] Frackowiak, E.; Khomenko, V.; Jurewicz, K.; Lota, K.; Béguin., F. Supercapacitors based on conducting polymers/nanotubes composites. *J. Power Sources.* **2006,** 153, 413–418.

[31] Gao, Y. Graphene and Polymer Composites for Supercapacitor Applications: a Review. *Nanoscale Res. Lett.* **2017,** 12, 387-404.

[32] Han, Y.; Ding, B.; Tong, H.; Zhang, X. Capacitance Properties of Graphite Oxide/Poly(3,4-ethylene

dioxythiophene) Composites. *J. Appl Polym Sci.* **2011,** 121, 892–898.

[33] Azman, N.H.N.; Lim, H.N.; Sulaiman, Y. Effect of Electropolymerization Potential on the Preparation of PEDOT/Graphene Oxide Hybrid Material for Supercapacitor Application. *Electrochim. Acta* **2016**, *188*, 785–792.

[34] Chang, J.-K.; Huang, C.-H. Tsai, W.-T.; Deng, M.-J. Sun, I.-W.; Chen, P.-Y. Manganese Films Electrodeposited at Different Potentials and Temperatures in Ionic Liquid and Their Application as Electrode Materials for Supercapacitors. *Electrochim. Acta.* **2008**, *53(13), 4447-4453*.

[35] Mele, C.; Catalano, M.; Taurino, A.; Bozzini, B. Electrochemical Fabrication of Nanoporous Gold-Supported Manganese Oxide Nanowires Based on Electrodeposition from Eutectic Urea/Choline Chloride Ionic Liquid. *Electrochim. Acta.* **2013**, *87*, 918–924.

[36] Rajesh, M.; Raj, C.J.; Manikandan, R.; Kim, B.C.; Park, S.Y.; Yu, K.H. A High Performance PEDOT/PEDOT Symmetric Supercapacitor by Facile in-Situ Hydrothermal Polymerization of PEDOT Nanostructures on Flexible Carbon Fibre Cloth Electrodes. *Mater. Today Energy.* **2017**, *6*, 96–104.

[37] Chang, J. K.; Huang, C. H.; Lee, M.T.; Tsai, W.T.; Deng, M.J.; Sun, I. W. Physicochemical factors that affect the pseudocapacitance and cyclic stability of Mn oxide electrodes. *Electrochim. Acta.* **2009**, 54, 3278-3284.

[38] Bozzini, B.; Gianoncelli, A.; Kaulich, B.; Mele, C.; Prasciolu, M.; Kiskinova, M. Electrodeposition of manganese oxide from eutectic urea/choline chloride ionic liquid: an in situ study based on soft X-ray spectromicroscopy and visible reflectivity. *J.Power Sources.* **2012**, 211, 71-76.

[39] Ryu, K. S.; Lee, Y. G.; Hong, Y. S.; Park, Y. J.; Wu, X. L.; Kim, K. M.; Kang, M. G; Park, N. G. Poly (ethylenedioxythiophene)(PEDOT) as polymer electrode in redox supercapacitor. *Electrochim. Acta.* **2004**, 50, 843-847.

[40] Sharma, R. K.; Zhai,. Multiwall carbon nanotube supported poly (3, 4 ethylenedioxythiophene)/manganese oxide nano-composite electrode for super-capacitors. L. *Electrochim. Acta.* **2009**, 54, 7148-7155.

[41] Huang, H.; Xia, L.; Zhao, Y.; Zhang, H.; Cong, T.; Wang, J.; Wen, N.; Yang, S.; Fan, Z.; Pan, L. Three-dimensional porous reduced graphene oxide/PEDOT:PSS aerogel: Facile preparation and high performance for supercapacitor electrodes. *Electrochim. Acta* **2020**, 364, 137297 (1-11).

[42] Bianchi, M.; Carli, S.; Di Lauro, M.; Prato, M.; Murgia, M.; Fadiga, L.; Biscarini, F. Scaling of Capacitance of PEDOT:PSS: Volume vs. Area. *J. Mater. Chem. C.* **2020**, *8*, 11252–11262.

[43] Ke, Q.; Wang, J. Graphene-Based Materials for Supercapacitor Electrodes. A Review. *J Mater.* **2016**, *2*, 37–54.

[44] Bozzini, B.; Mele, C.; D'Urzo, L. Electrodeposition of Cu from Acidic Sulphate Solutions in the Presence of PEG - Part II Visible Electroreflectance Spectroscopy Measurements during Electrodeposition. *J. Appl. Electrochim.* **2016**, *36*, 87–96.